RSC Advances

PAPER

View Article Online
View Journal | View Issue

Cite this: *RSC Adv.*, 2022, **12**, 4042

Individual iron(III) glycerolate: synthesis and characterisation†

Tat'yana G. Khonina, *[a] Elena Yu. Nikitina,[a] Alexander Yu. Germov,[b] Boris Yu. Goloborodsky,[b] Konstantin N. Mikhalev,[b] Ekaterina A. Bogdanova,[c] Denis S. Tishin,[a] Alexander M. Demin,[a] Victor P. Krasnov,[a] Oleg N. Chupakhin[ad] and Valery N. Charushin[ad]

Received 19th November 2021
Accepted 25th January 2022

DOI: 10.1039/d1ra08485b

rsc.li/rsc-advances

Iron(II) and iron(III) salts of strong acids form iron glycerolates on heating at 180 °C with glycerol in the presence of an equivalent amount of alkali. Individual iron(III) glycerolate was obtained for the first time. When Fe_3O_4 magnetic nanoparticles were heated with glycerol, an iron(III) glycerolate shell was formed on their surface.

Currently, glycerolates of various metals (Ti, Co, Fe, Zn, *etc.*) are used as catalytic systems[1,2] or as precursors to obtain nanoparticles, including iron oxide magnetic nanoparticles (MNPs),[3] and nanostructure materials for technical and biomedical applications.[4–8]

Glycerolates of biogenic elements (Si, Zn, B and Ti) are of particular interest because of their biological activity. They are used as biocompatible precursors in the sol–gel synthesis of pharmacologically active hydrogels with reparative, regenerative, antioxidant, immunotropic and antimicrobial effects.[8–10] In this regard, glycerolate of the biogenic iron element can be considered as an innovative biocompatible precursor in the sol–gel synthesis of composite bioactive hydrogels possessing a haemostatic effect characteristic of various iron compounds.[11]

A promising trend in biomedicine is the core–shell modification of Fe_3O_4 MNPs for MRI diagnostics or magnetic hyperthermia of tumors.[12–14] So, the development of an iron glycerolate shell on the surface of Fe_3O_4 MNPs[15] and studying an opportunity of using modified nanoparticles in magnetic hyperthermia is of particular interest. In addition, the antibacterial activity of Fe_3O_4 MNPs with glycerol adsorbed on the surface was also demonstrated.[16,17]

In the literature, individual iron(II) and iron(III) glycerolates have not so far been described. At the same time, the synthesis of individual forms is extremely important for biomedical purposes in order to determine bioavailability parameters. The available literature data concern only mixed iron(II,III) glycerolate that is usually formed as a result of the interaction of di- or trivalent iron oxides, hydroxides or salts (mainly oxalates) with glycerol at elevated temperatures (up to 245 °C).[15,18–20] It is worth noting that all attempts to synthesize iron glycerolates from chlorides and sulfates of ferrous or ferric irons proved to be unsuccessful.[20] At the same time, iron glycerolate was obtained from iron(III) nitrate in boiling glycerol under reflux (280 °C);[3] however, contents of iron(III) and iron(II) were not determined in that product.

Regardless of the iron valence state in the starting compound, Fe(II) and Fe(III) are present in the resulting glycerolate in all cases. It should be noted that the possible pathways of the redox process for obtaining mixed iron(II,III) glycerolate are not discussed in the literature. The quantitative Fe(II)/Fe(III) ratio is usually determined by the Mössbauer spectroscopy[21] or the colorimetric method.[19] The composition of iron(II,III) glycerolate is mainly described by the following formulas: $Fe_2C_6H_{11}O_6$ (powder diffraction file JCPDSD-ICDD PDF 2, card [23-1731])[18] and $Fe_3^{+2}Fe_2^{+3}(C_3H_5O_3)_4$.[19–21] It was not possible to obtain single crystals of iron glycerolate and calculate the unit cell parameters.[4,18]

We have found that the reactions of iron(II) or iron(III) chlorides and sulfates with glycerol proved to proceed only in the presence of an equivalent amount of alkali to give glycerolates of various chemical compositions. Thus, for the first time, individual iron(III) glycerolate $FeC_3H_5O_3$ (**1**) was obtained in 91% yield on heating iron(III) chloride hexahydrate $FeCl_3 \cdot 6H_2O$ with sodium hydroxide in an excess of glycerol $C_3H_8O_3$ at 180 °C for 18 h (Scheme 1) (see ESI†).

The resulting product **1** is a light green powder insoluble in water and organic solvents, thus indicating a probable polymeric structure. It should be noted that the reaction temperature (180 °C) and duration (18 h) appear to be optimal taking into account a high yield of the product and its purity.

[a]*Postovsky Institute of Organic Synthesis, Russian Academy of Sciences, Ural Branch, Yekaterinburg 620108, Russia. E-mail: khonina@ios.uran.ru*

[b]*Miheev Institute of Metal Physics, Russian Academy of Sciences, Ural Branch, Yekaterinburg 620108, Russia*

[c]*Institute of Solid State Chemistry, Russian Academy of Sciences, Ural Branch, Yekaterinburg 620108, Russia*

[d]*Institute of Chemical Technology, Ural Federal University, Yekaterinburg 620002, Russia*

† Electronic supplementary information (ESI) available. See DOI: 10.1039/d1ra08485b

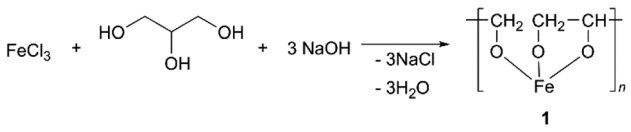

Scheme 1 Synthesis of iron(III) glycerolate **1**.

Heating iron(II) sulfate heptahydrate $FeSO_4 \cdot 7H_2O$ in glycerol in the presence of an equivalent amount of NaOH under the same conditions (180 °C, 18 h) resulted in mixed iron(II,III) glycerolate $Fe_3^{+2}Fe_5^{+3}(C_3H_5O_3)_7$ (**2**) in 83% yield (see ESI†). The resulting product is a dark green powder that is poorly soluble in water and organic solvents.

Iron glycerolates **1** and **2** were formed as colored powders; they are storage stable with no change in structure and no noticeable change in color; they do not melt to decomposition temperature. Dilute acids or hot water caused decomposition with the production of glycerol and iron (hydroxy)oxides or salts, as it was noted earlier.[18] Plausible pathways for the formation of iron glycerolate **1**, as well as iron glycerolate **2** (Scheme 2) and the features of the process are discussed below.

Magnetic materials based on Fe_3O_4 nanoparticles with a biologically compatible coating are of great interest for biology and medicine.[12–14] Previously, we were the first to demonstrate the possibility of forming a shell of iron glycerolate on the surface of Fe_3O_4 MNPs by a simple and reproducible method, namely, by interacting Fe_3O_4 MNPs with glycerol at 220 °C for 40 h.[15] In this work, we optimized the synthetic procedure and chose the optimum conditions (180 °C, 18 h) (see ESI†). The composition of the resulting shell was found to correspond to iron glycerolate **1**.

To determine the Fe(II)/Fe(III) ratio in the obtained products, we used the Mössbauer spectroscopy. Fig. 1 shows the Mössbauer spectra of iron glycerolates **1** (a and c) and **2** (b). The samples were prepared by deposition of the powder onto aluminum foil with a diameter of 22 mm (see ESI†).

The Mössbauer spectrum of iron glycerolate **1** (Fig. 1a) contains only one doublet (red line) with quadrupole splitting value of 0.48 mm s^{-1} (Table 1) which is typical for Fe(III) positions,[21] at the same time there are no signals typical for Fe(II). The Mössbauer spectrum of iron glycerolate **2** (Fig. 1b) contains two doublets (red and blue lines) with quadrupole splitting Q_s values of 0.46 and 2.29 mm s^{-1} (Table 1) corresponding to Fe(III) and Fe(II) positions, respectively.[21] In this case, the content of Fe(II) was 38%; Fe(III), 62%.

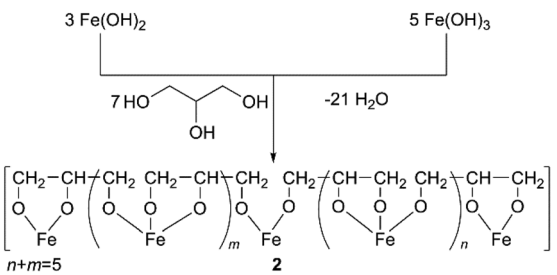

Scheme 2 Formation of iron(II,III) glycerolate **2**.

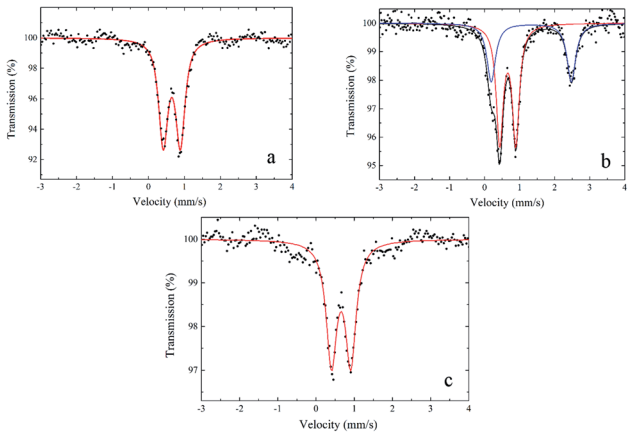

Fig. 1 ^{57}Fe Mössbauer spectra at 295 K of (a) iron(III) glycerolate **1**, (b) iron(II,III) glycerolate **2**, and (c) iron(III) glycerolate **1** from Fe_3O_4 MNPs. The doublets of Fe^{3+} and Fe^{2+} ions are marked in red and blue, respectively. The black line represents the sum of these lines. Sodium nitroprusside $C_5FeN_6Na_2O$ was taken as reference.

The Mössbauer spectrum of a sample obtained from Fe_3O_4 MNPs (Fig. 1c) also contains a doublet (red line) with Q_s = 0.51 mm s^{-1} (Table 1) characteristic of Fe(III). Any signals typical for Fe(II) are absent, which confirms the presence of a shell of iron glycerolate **1**. It should be noted that the signals of Fe(II) contained in the core of the Fe_3O_4 MNPs were not recorded under these conditions of spectrum registration.

The results of the quantitative determination of Fe(II) and Fe(III) by the Mössbauer spectroscopy in the studied products, as well as the data of their elemental analyses (Table 2), allowed us to propose the molecular formulas for iron glycerolates **1** and **2**. Elemental compositions of the synthesized samples were determined on a CHN analyzer, the Fe content was calculated from the amount of incombustible residue (Fe_2O_3). The elemental composition of glycerolate **1** is in good agreement with the molecular formula $FeC_3H_5O_3$ and practically does not differ from the elemental composition calculated for iron glycerolate $Fe_2C_6H_{11}O_6$ (card [23-1731]).

It should be noted that the experimentally determined Fe content (%) in iron(II,III) glycerolate[18] proved to differ considerably from the calculated composition for the formula $Fe_2C_6H_{11}O_6$. At the same time, the experimental results for iron(II,III) glycerolate[19] are in good agreement with the formula $Fe_3^{+2}Fe_2^{+3}(C_3H_5O_3)_4$. The data of elemental analyses for the mixed iron glycerolate **2** obtained in this study correspond to the formula $Fe_3^{+2}Fe_5^{+3}(C_3H_5O_3)_7$. However, both mixed iron glycerolates differ significantly in their compositions. Thus, the chemical compositions of iron glycerolates differs significantly depending on the nature of the starting compounds and reaction conditions.

Fig. 2 shows the X-ray diffraction (XRD) spectra of the powders of (a) iron glycerolate **1**, (b) iron glycerolate **2**, and (c) Fe_3O_4 MNPs with a shell of iron(III) glycerolate **1**. All spectra contain peak at 12.7 deg. 2θ (8.1 Å), which is the main diffraction line of iron glycerolate.[18]

Table 1 Fitting parameters of ^{57}Fe Mössbauer spectra (Fig. 1) for iron glycerolates

Sample	Starting material	Spectral lines	Isomer shift, δ_{iso} (mm s^{-1})	Q_S (mm s^{-1})	Relative content (%)	Line width (mm s^{-1})
Iron(III) glycerolate **1** (a)	$FeCl_3 \cdot 6H_2O$	Fe^{3+}	0.66	0.48	100	0.31
Iron(III) glycerolate **1** (c)	Fe_3O_4 MNPs	Fe^{3+}	0.66	0.51	100	0.33
Iron(II,III) glycerolate **2** (b)	$FeSO_4 \cdot 7H_2O$	Fe^{3+}	0.66	0.46	62	0.24
		Fe^{2+}	1.33	2.29	38	0.30

Table 2 Elemental composition of iron glycerolates

	Composition (%)					
	Experimental			Calculated		
Iron glycerolate	C	H	Fe	C	H	Fe
$FeC_3H_5O_3$ (**1**)	24.75	3.44	38.40	24.86	3.48	38.54
$Fe_2C_6H_{11}O_6$[a]	24.70	3.25	41.00	24.78	3.81	38.40
$Fe_3^{+2}Fe_2^{+3}(C_3H_5O_3)_4$[b]	22.47	3.31	43.69	22.68	3.17	43.94
$Fe_3^{+2}Fe_5^{+3}(C_3H_5O_3)_7$ (**2**)	23.12	3.20	41.89	23.66	3.48	41.22

[a] Iron(II,III) glycerolate synthesized from goethite in boiling glycerole.[18] [b] Iron(II,III) glycerolate synthesized from goethite, lepidocrocite, hematite at 245 °C.[19]

Fig. 3 shows HRTEM images of (a) starting Fe_3O_4 MNPs and (b) Fe_3O_4 MNPs coated with iron glycerolate **1**. The modified Fe_3O_4 MNPs had a core–shell structure with an average magnetite core size of 10 nm coated with an iron glycerolate shell 2–4 nm thick.

Fig. 4 shows the IR spectra of (a) iron glycerolate **1**, (b) iron glycerolate **2**, (c) Fe_3O_4 MNPs, and (d) MNPS coated with glycerolate **1**. The most intensive bands at 2850–2840 cm^{-1} correspond to the stretching vibration of C–H bonds. The bands in the range 1480–1200 cm^{-1} are attributed to the deformation vibrations of C–H bonds. The high intensity bands in the ranges 1150–880 and 780–690 cm^{-1} can be assigned to deformation vibrations of C–O–Fe groups in glycerolate fragments. Band at 537 cm^{-1} is characteristic of the initial Fe_3O_4 MNPs. In modified nanoparticles, it is likely to be shifted to 582 cm^{-1} and superimpose on the bands in the range 600–610 cm^{-1} corresponding to C–O–Fe vibrations. It should be noted that the IR spectrum of modified Fe_3O_4 MNPs is similar in position and shape of absorption bands to the spectrum of glycerolate **1**. Our measurements are in agreement with the previous IR studies of iron glycerolates.[3,15,21]

Thus, the IR and XRD spectra of iron glycerolates **1** and **2** turned out to be similar. Therefore, the quantitative determination of Fe(II) and Fe(III) contents in iron glycerolates **1** and **2** proved to be possible only by using the Mössbauer spectroscopy. The results obtained have allowed us to refine the information on the composition of iron glycerolate available in the XRD database [card 23-1731].[18]

Considering the possible pathways for the formation of iron glycerolates **1** and **2**, it can be assumed that the process includes the ion exchange reaction between iron salts and alkali with the formation of amorphous iron(III) and iron(II) hydroxides, respectively. In this case, iron(II) hydroxide is partially oxidized by atmospheric oxygen to iron(III) hydroxide; however, the reduction of iron(III) to iron(II) with glycerol does not occur under the reaction conditions. Then iron(II) and iron(III) hydroxides enter the reversible condensation reaction with glycerol to form iron glycerolates. As noted above, the resulting products are hydrolysed in hot water, which corresponds to a shift in the equilibrium in the condensation reaction towards the starting materials. However, an excess of glycerol and removal of water when the reaction mixture is heated up to 180 °C leads to a shift in the equilibrium towards the reaction products, as evidenced by their high yields.

Thus, iron glycerolate **1** is formed from iron(III) hydroxide when the latter is reacted with glycerole (Scheme 1); iron glycerolate **2** is formed from iron(II) and iron(III) hydroxides (Scheme

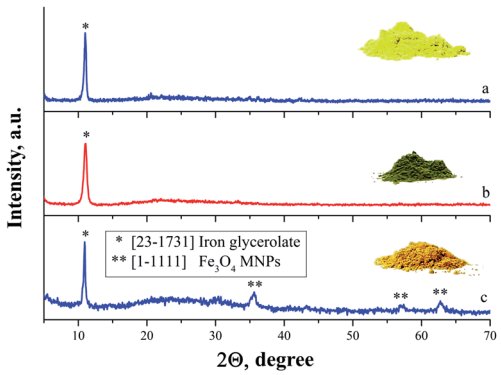

Fig. 2 X-ray diffraction spectra of (a) iron(III) glycerolate **1**, (b) iron(II,III) glycerolate **2**, (c) Fe_3O_4 MNPs coated with glycerolate **1**. In the insets: photos of the analysed powders.

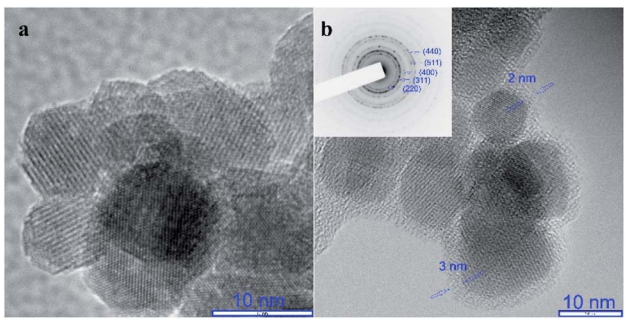

Fig. 3 HRTEM images of (a) starting Fe_3O_4 MNPs Fe_3O_4 and (b) MNPs coated with iron glycerolate **1**; in inset, an electron diffraction pattern.

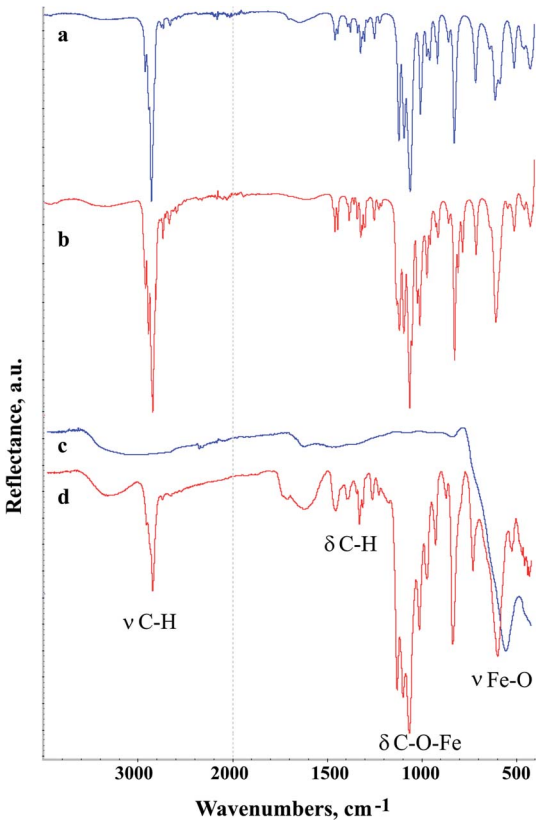

Fig. 4 (a) IR spectra of (a) iron(III) glycerolate **1**, (b) iron(II,III) glycerolate **2**, (c) Fe_3O_4 MNPs and (d) MNPs coated with glycerolate **1**.

2). The graphical formula of iron glycerolate **2** is represented as a conditional notation corresponding to the molecular formula $Fe_3^{+2}Fe_5^{+3}(C_3H_5O_3)_7$. When $m = n = 1$, the graphical formula does correspond to the molecular formula $Fe_3^{+2}Fe_2^{+3}(C_3H_5O_3)_4$ (ref. 21) in iron glycerolate **2**, $Fe_3^{+2}Fe_2^{+3}(C_3H_5O_3)_4 \cdot 3FeC_3H_5O_3$. It should be noted that all our attempts to synthesize individual iron(II) glycerolate have failed, even in an inert gas atmosphere.

It should be noted that the formation of iron hydroxides and, consequently, iron glycerolates does not occur without alkali, since the hydrolysis of iron salts of strong acids proceeds stepwise and results mainly in the formation of basic salts as the first step of the hydrolysis process. In addition, we cannot exclude that sodium monoglycerolate derived from equilibrium interaction of NaOH with an excess of glycerol is also involved in the formation of iron glycerolates **1** and **2**. Sodium monoglycerolate, like NaOH, can enter the ion exchange reaction with iron salts with the formation of glyceroxy iron derivatives.

The proposed chemistry of the process, in our opinion, is characteristic of all iron(II) and iron(III) salts of strong acids.

$$2\,Fe(OH)_3 + H_2C_2O_4 \longrightarrow 2\,Fe(OH)_2 + 2CO_2 + 2\,H_2O \quad (1)$$

$$Fe(OH)_3 + C_3H_8O_3 \longrightarrow Fe(OH)_2 + \underset{\text{products}}{\text{glycerol oxidation}} + H_2O \quad (2)$$

Scheme 3 Reduction of iron(III) hydroxide with oxalic acid (**1**) or glycerol (**2**).[19]

It is known that iron salts of weak acids, for example, iron(II) oxalate (as dihydrate $FeC_2O_4 \cdot 2H_2O$) or iron(III) oxalate (as pentahydrate $Fe_2(C_2O_4)_3 \cdot 5H_2O$) are capable of reacting with glycerol without alkali at 240 °C to form mixed iron(II,III) glycerolate $Fe_3^{+2}Fe_2^{+3}(C_3H_5O_3)_4$.[21] It is interesting to note that the chemical composition of iron(II,III) glycerolate is the same in both cases. It can be assumed that complete hydrolysis of these salts takes place, which is facilitated by an increased temperature, thus resulting in the formation of iron(II) or iron(III) hydroxides and oxalic acid. At the same time, in cases of FeC_2O_4 (as well as $FeSO_4$), the formed iron(II) hydroxide is partially oxidized by atmospheric oxygen to give iron(III) hydroxide. Iron(II) and iron(III) hydroxides are supposed to react further with glycerol to form a mixed iron(II,III) glycerolate. We believe that in the case of $Fe_2(C_2O_4)_3$, the formed iron(III) hydroxide is reduced by oxalic acid, which is also the product of hydrolysis, to iron(II) hydroxide (Scheme 3, reaction 1). Further, when reacting with glycerol, a mixture of iron(II) and iron(III) hydroxides is expected to form a mixed iron(II,III) glycerolate. In our opinion, the reduction with glycerol (Scheme 3, reaction 2), according to the work,[19] cannot be considered as the determining process.

At the same time, to the best of our knowledge there are scarcely available data on oxidation of glycerol on reacting with iron(III) salts. It has been established,[19] that a carbonyl compound is present in the reaction mixture, as indicated by a low intensity CO stretching vibrational band. However, qualitative tests carried out to determine the character of the CO function proved to be negative for aldehydes and ketones.

Thus, the key difference in the pathways for obtaining iron glycerolates from iron(II) or (III) salts of strong or weak acids is associated with the step of the formation of iron hydroxides: in case of iron salts of strong acids, iron hydroxides are formed due to the ion exchange reaction of iron salts with alkali, while iron salts of weak acids undergo their complete hydrolysis.

In summary, it has first been shown that iron(II) and iron(III) salts of strong acids ($FeCl_3$, $FeSO_4$) are able to form iron glycerolates. The previously undescribed individual iron(III) glycerolate $FeC_3H_5O_3$ was obtained from $FeCl_3$ as an example, glycerol and NaOH at 180 °C in one-pot synthesis. It has been found that due to the direct interaction of Fe_3O_4 MNPs with glycerol at 180 °C, an iron(III) glycerolate shell is formed on the nanoparticle surface. The obtained iron glycerolates were characterized by Mössbauer and IR spectroscopy, XRD and elemental analysis.

Individual iron(III) glycerolate can be considered as a novel biocompatible precursor in the sol–gel synthesis of pharmacologically active nanocomposite materials and for further preparation of advanced composite magnetic nanomaterials with glycerolate shell to be used in magnetic hyperthermia of tumors. In addition, it can be used as a precursor for in the preparation of MNPs and as a catalyst for various chemical processes.

Conflicts of interest

There are no conflicts to declare.

Acknowledgements

The work was carried out with financial support from the Ministry of Science and Higher Education of the Russian Federation (grant 075-15-2020-777) using the equipment of the Centre for Joint Use "Spectroscopy and Analysis of Organic Compounds" at the Postovsky Institute of Organic Synthesis of UB RAS. Mössbauer spectroscopy, XRD, and HRTEM studies were carried out within the state programs of Miheev Institute of Metal Physics of UB RAS («Function»), Institute of Solid State Chemistry of UB RAS, and Ural Federal University, correspondingly. Authors are grateful to Dr Maksim S. Karabanov (Ural Center for Shared Use "Modern Nanotechnology" at the Ural Federal University) for HRTEM study.

References

1 M. Wang, J. Jiang and L. Ai, *ACS Sustainable Chem. Eng.*, 2018, **6**, 6117–6125.
2 P. C. Lau, T. L. Kwong and K. F. Yung, *Sci. Rep.*, 2016, **6**, 23822.
3 V. Bartůněk, D. Průcha, M. Švecová, P. Ulbrich, S. Huber, D. Sedmidubský and O. Jankovský, *Mater. Chem. Phys.*, 2016, **180**, 272–278.
4 J. Zhao, Y. Liu, M. Fan, L. Yuan and X. Zou, *Inorg. Chem. Front.*, 2015, **2**, 198–212.
5 H. Dong and C. Feldmann, *J. Alloys Compd.*, 2012, **513**, 125–129.
6 O. Jankovský, V. Rach, D. Sedmidubský, S. Huber, P. Ulbrich, M. Svecova and V. Bartunek, *J. Alloys Compd.*, 2017, **723**, 58–63.
7 M. Y. Cheong, A. H. Hazimah, A. A. H. Zafarizal and I. Rosnah, *J. Oil Palm Res.*, 2012, **24**, 1287–1295.
8 T. G. Khonina, A. P. Safronov, E. V. Shadrina, M. V. Ivanenko, A. I. Suvorova and O. N. Chupakhin, *J. Colloid Interface Sci.*, 2012, **365**, 81–89.
9 T. G. Khonina, M. V. Ivanenko, O. N. Chupakhin, A. P. Safronov, E. A. Bogdanova, M. S. Karabanalov, V. V. Permikin, L. P. Larionov and L. I. Drozdova, *Eur. J. Pharm. Sci.*, 2017, **107**, 197–202.
10 T. G. Khonina, N. V. Kungurov, N. V. Zilberberg, N. P. Evstigneeva, M. M. Kokhan, A. I. Polishchuk, E. V. Shadrina, E. Yu. Nikitina, V. V. Permikin and O. N. Chupakhin, *J. Sol–Gel Sci. Technol.*, 2020, **95**, 682–692.
11 M. T. Matter, F. Starsich, M. Galli, M. Hilber, A. A. Schlegel, S. Bertazzo, S. E. Pratsinis and I. K. Herrmann, *Nanoscale*, 2017, **9**, 8418–8426.
12 N. D. Thorat, H. E. Townley, R. M. Patil, S. A. M. Tofail and J. Bauer, *Drug Discovery Today*, 2020, **25**, 1245–1252.
13 A. M. Demin, A. G. Pershina, A. S. Minin, O. Y. Brikunova, A. M. Murzakaev, N. A. Perekucha, A. V. Romashchenko, O. B. Shevelev, M. A. Uimin, I. V. Byzov, D. Malkeyeva, E. Kiseleva, L. V. Efimova, S. V. Vtorushin, L. M. Ogorodova and V. P. Krasnov, *ACS Appl. Mater. Interfaces*, 2021, **13**, 36800–36815.
14 A. M. Demin, A. V. Maksimovskikh, A. V. Mekhaev, D. K. Kuznetsov, A. S. Minin, A. G. Pershina, M. A. Uimin, V. Y. Shur and V. P. Krasnov, *Ceram. Int.*, 2021, **47**, 23078–23087.
15 A. M. Demin, T. G. Khonina, E. V. Shadrina, E. A. Bogdanova, D. K. Kuznetsov, A. V. Mekhaev, V. Ya Shur and V. P. Krasnov, *Russ. Chem. Bull.*, 2019, **68**, 1178–1182.
16 C. L. Popa, A. M. Prodan, P. Chapon, C. Turculet and D. Predoi, *J. Nanomater.*, 2015, 465034.
17 A. M. Prodan, M. Beuran, C. S. Turculet, M. Popa, E. Andronescu, C. Bleotu, S. M. Raita, M. Soare and O. Lupescu, *Rom. Biotechnol. Lett.*, 2018, **23**, 13901–13908.
18 E. W. Radoslovich, M. Raupach, P. G. Slade and R. M. Taylor, *Aust. J. Chem.*, 1970, **23**, 1963–1970.
19 P. F. Fuls, L. Rodrique and J. J. Fripiat, *Clays Clay Miner.*, 1970, **18**, 53–62.
20 L. Rodrique, G. Delvaux and A. Dardenne, *Powder Technol.*, 1978, **19**, 93–101.
21 P. Bruylants, A. Munaut, G. Poncelet, J. Ladriere, J. Meyers and J. Fripiat, *J. Inorg. Nucl. Chem.*, 1980, **42**, 1603–1611.